IEEE Access
Multidisciplinary | Rapid Review | Open Access Journal

Received May 11, 2017, accepted May 29, 2017, date of publication June 2, 2017, date of current version July 17, 2017.

Digital Object Identifier 10.1109/ACCESS.2017.2711533

On the Optimization of Iterative Clipping and Filtering for PAPR Reduction in OFDM Systems

KELVIN ANOH[1], (Member, IEEE), CAGRI TANRIOVER[2], AND BAMIDELE ADEBISI[1], (Senior Member, IEEE)

[1]School of Engineering, Manchester Metropolitan University, Manchester M1 5GD, U.K.
[2]Intel Corporation, Hillsboro, OR 97124, USA

Corresponding author: Kelvin Anoh (k.anoh@mmu.ac.uk)

This work was supported in part by the Smart In-Building Micro Grid for Energy Management Project through EPSRC under Grant EP/M506758/1 and in part by the Innovate U.K. Project under Grant 101836.

ABSTRACT Orthogonal frequency division multiplexing (OFDM) offers spectral efficiency advantage, however, it is limited by peak-to-average power (PAPR) problem. The PAPR can be reduced using iterative clipping and filtering (ICF) scheme but requires that the same signals are iteratively clipped with a fixed clipping threshold at different clipping iterations. This method warrants that fast-Fourier transform (FFT)/inverse FFT (IFFT) blocks must be driven in the order of iterations many times to attain a desired PAPR threshold which expends the system power and expands the processing time. Using a second-order cone program, the number of iterations required to attain the desired PAPR threshold was reduced. This optimized ICF (OICF) was later simplified using Lagrange multiplier (LM). In this paper, we apply an adaptive clipping threshold to the LM scheme to improve the performance of the simplified OICF (SOICF). Our results show significant reduction of the PAPR problem compared with the earlier SOICF scheme albeit with some degradation in the bit error ratio (BER) performance that can be under 1.0 dB depending on the chosen clipping threshold. In addition, we also illustrate the results of the performances and the theoretical relationships between the error vector magnitude (EVM) and PAPR, between clipping ratio (CR) and EVM, and lastly the inter-dependencies of EVM, PAPR, the number of OFDM subcarriers, and the CR.

INDEX TERMS PAPR, OFDM, Optimization, Iterative clipping and Filtering (ICF), Adaptive, Lagrange Multiplier.

I. INTRODUCTION

Since 1971 when it was shown that discrete Fourier transform (DFT) could be used to partition wide-bandwidths into parallel and orthogonal subcarriers [1], the use of orthogonal frequency division multiplexing (OFDM) realized from the DFT has been widely adopted in the design of modern communication systems [2]. The trend has also motivated the study of other transforms for multicarrier application such as wavelets [3]. This is due to its ability to increase throughput by multiplexing large streams of data over any constrained bandwidth by partitioning them into parallel adjacent subcarriers. By this fact, the symbol time is increased so that the system becomes robust over fading channels. One problem prevails from such architecture, for example, the subcarriers subtend non-uniformly distributed peaks so that the peak-to-average power (PAPR) becomes high. Evidently, these peaks drive the power amplifiers of OFDM systems to operate near the saturation region [4].

Meanwhile, the high power amplifiers (HPA) used in base stations are responsible for the significant share of the energy costs in a communication system [5]. The energy efficiency of the HPA is directly related to the PAPR of the input signal, which is particularly important in OFDM multicarrier transmission [6]. Also, as acknowledged in [6], high PAPR is the key reason why OFDM is not adopted in the uplink of mobile communication standards whilst putting constraints on the downlink coverage due to output power limitations.

There are several methods that can be used to combat this problem in literature; these can be grouped into signal distortion techniques, multiple signaling and probabilistic techniques, and coding techniques [2]. Iterative clipping is one of the simplest widely known techniques from the amplitude distortion family for PAPR reduction technique. Its major drawback is that the deliberately clipped OFDM symbol peaks impact the noise overhead of the system and

so reduces the bit error ratio (BER). Since the clipping also involves oversampling, this leads to out-of-band power emission. However, a frequency domain filtering helps to eliminate the noise and the out-of-band power; this however culminates into peak-regrowth and leads to increase in PAPR [7]. Thus, modern techniques involve iterative clipping and filtering (ICF) [2], [4], [8]–[10].

In [11], it was shown that the ICF technique expends the system resources in the order of the iterations in driving the IFFT/FFT blocks. Reducing the number of iterations to achieve a PAPR target would also reduce the device resources lost to the ICF process. Gurung *et al.* [12] make the assumption that the clipped peaks are assumed to be parabolic pulses. While this is true if the clipping threshold is large, this method does not work for low clipping thresholds, which is also acknowledged by the authors. In our approach, no assumption on the characteristics of the clipped peaks are made and therefore the concept is universally applicable in OFDM systems. Consequently, [4] showed a method that optimizes the process by using the widely-adopted convex optimization algorithm based on second-order cone program (SOCP) solvable by the MATLAB-enabled CVX optimization software [13]. In that work, the authors referred to their solution as optimized ICF (OICF) [4]. Zhu *et al.* [8] later acknowledged the OICF approach to be expensive in terms of system design due to the complexity involved in constructing an optimal filter using the CVX tool. To overcome this problem, a new optimal method that constructs a PAPR-vector to minimize the error vector magnitude (EVM) was then proposed and solved by using Lagrange Multiplier optimization (LMO) [8]. The latter achieved significant reduction in the resources consumed during the optimization of ICF process reducing the $\mathcal{O}\left(N^3\right)$ computations of [4] to only $\mathcal{O}\left(N\right)$ computations.

The fundamental problem with both OICF and SOICF is that they are based on fixed clipping threshold. Earlier, Lee and Kim [14] proposed an adaptive ICF (AICF) technique of improving the PAPR reduction limit of the conventional ICF process through some adaptive determination of near crest factor and thus new reduction limit peaks. That study significantly improved the PAPR of an iteratively clipped and filtered OFDM signal using the adaptive clipping ratio. To enhance the performance of the novel SOICF, we proposed an adaptive SOICF technique that overcomes the PAPR performance limit of the present SOICF with no additional design cost as it will be demonstrated shortly. The method we propose combines the strengths of SOICF and AICF to improve PAPR reduction and optimally utilize the available communication device resources. Our result show an improved performance over the current SOICF technique as it will be shown in Section III. Wang *et al.* [14], applied genetic algorithm (GA) for adaptive reserved tone ICF (ART-ICF) which is computationally rigorous and expends lots of processing resources whilst increasing input-output latency as it involves an exhaustive search for adaptive step sizes. In fact, Wang and Xiao in [15] showed an improved method of solving the problem by using differential evolution. Meanwhile, both the ART-ICF and the improved version all suffer from the exhaustive search problem of GA. Nandalal and Sophia [9] proposed the use of custom conic optimization with AICF, unfortunately, the method was based on the CVX public software [13] which consumes device power and the requires up to four iterations to obtain a good BER performance. In this study, we improve the works done in [8], [14], and [9]. It is worthy to mention here that the earliest work on the construction of optimal filter proposed in [4] which involved the construction filter using CVX was also independently similarly addressed in [16] although based on graded bandlimiting filter.

The rest of this paper is organized as follow; we formulate the problem in Section II and perform the system evaluation in Section III. The results are also discussed in Section III followed by the conclusion.

II. PROBLEM FORMULATION

OFDM divides a wideband into many parallel orthogonal subcarriers in the order of the DFT size used, say N. These orthogonal subcarriers convey data frames $\boldsymbol{D} = [\boldsymbol{d}_1, \boldsymbol{d}_2, \cdots, \boldsymbol{d}_P]$, where $\boldsymbol{d}_p = [d_0, d_1, \cdots, d_{N-1}]^T \ \forall p = 1, 2, \cdots, P$ and $[\cdot]^T$ represents the complex conjugate of $[\cdot]$. In frequency domain these data symbols are processed using the DFT to realize $\boldsymbol{X}$; for simplicity we shall consider only one frame. Thus, consider an OFDM system with some frequency domain symbols such as $\bar{X}_p = \left[\bar{X}_0, \bar{X}_1, \cdots, \bar{X}_{N-1}\right]$. The frequency domain signal of length N is converted to time domain using an over-sized IDFT of order $LN = L \times N$ after some oversampling. With the oversampling, for example $X = \left[\bar{X}_0, \bar{X}_1, \cdots, \bar{X}_{N-1}, 0, 0, \cdots, 0_{N(L-1)}\right]$, its time domain equivalent can be represented as

$$\boldsymbol{x}(n) = \frac{1}{\sqrt{LN}} \sum_{k=0}^{LN-1} X(k) e^{j2\pi \frac{kn}{LN}} \ \forall n = 0, 1, \cdots, LN-1 \qquad (1)$$

where L is the oversampling factor and $X(k), \boldsymbol{x}(n) \in \mathbb{C}^{LN}$ with $\mathbb{C}$ representing the complex domain. This factor, L, follow from the fact that at Nyquist sampling rate, OFDM symbols may not demonstrate equivalent PAPR as the continuous-time signals [17], thus, the time domain signal must satisfy $L \geq 4$ [18]. Consider also that since the OFDM symbols are complex, so, the amplitude can be expressed as

$$|\boldsymbol{x}(n)| = \sqrt{\boldsymbol{x}_r(n)^2 + \boldsymbol{x}_i(n)^2} \qquad (2)$$

where $\boldsymbol{x}_r(n)$ and $\boldsymbol{x}_i(n)$ are real and imaginary parts, respectively, from $\boldsymbol{x}(n) = \boldsymbol{x}_r(n) + j\boldsymbol{x}_i(n)$. For an OFDM system with sufficiently large subcarriers (such as $N \geq 64$), the knowledge of the central limit theorem provides that the real and imaginary parts of $\boldsymbol{x}(n)$ are asymptotically independent and identical Gaussian distributed variables [19]. Put differently, the amplitudes ($|\boldsymbol{x}(n)|$) can be described using the probability

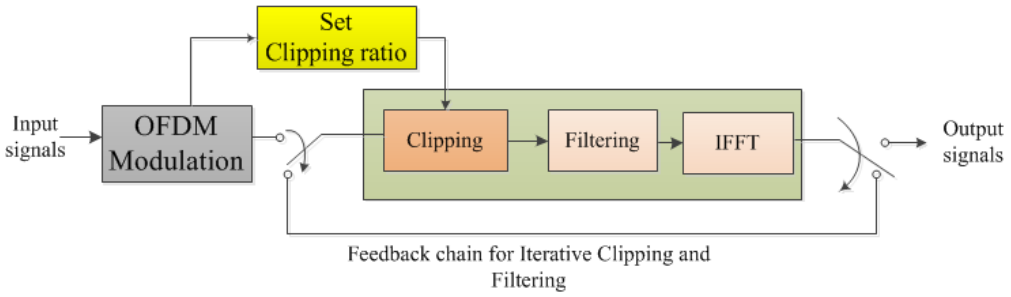

FIGURE 1. Conventional iterative clipping and filtering architecture for reducing the PAPR of OFDM signals based on static clipping ratio.

density function (PDF) of a Rayleigh distribution such as [19]

$$f_{|\boldsymbol{x}(n)|}(x_0) = \frac{x_0^2}{\sigma_x^2} \exp\left(-\frac{x_0^2}{2\sigma_x^2}\right), \quad \forall n = 0, 1, \cdots, LN-1 \tag{3}$$

where x_0 is the discrete-time envelope of $\boldsymbol{x}(n)$, σ_x^2 is the variance and $f_{|\boldsymbol{x}(n)|}(\cdot)$ is PDF. Being Rayleigh distributed, it is implied that the peak power of $\boldsymbol{x}(n)$ can be much larger than the average power leading to high PAPR metric which can adversely affect the OFDM system [8]. The PAPR can be defined as

$$\text{PAPR}\{\boldsymbol{x}(n)\} = 10\log_{10}\left\{\frac{\max\limits_{n=0,1,\cdots,LN-1}\left(|x(n)|^2\right)}{\frac{1}{LN}\sum\limits_{n=0}^{LN-1}\left(|x(n)|^2\right)}\right\}(dB). \tag{4}$$

The PAPR is usually measured using the cumulative density function (CDF) and it is related to the complementary CDF (CCDF) of $|\boldsymbol{x}(n)|$ as

$$\begin{aligned} CC_{|x|}(x_0) &= \Pr\{|\boldsymbol{x}(n)| > x_0\} \\ &= \int_0^x \frac{2y}{\sigma_x^2}\exp\left(-\frac{y^2}{\sigma_x^2}\right)dy \\ &= 1 - \exp\left(-\frac{x_0^2}{\sigma_x^2}\right), \quad \forall x_0 \geq 0 \end{aligned} \tag{5}$$

where $\Pr\{\cdot\}$ represents the probability of $\{\cdot\}$. It follows that, for $n = 0, 1, \cdots, LN-1$, $CC_{|x|}(x_0) = \left(1 - \exp\left(-\frac{x_0^2}{\sigma_x^2}\right)\right)^{LN}$, then the CCDF becomes $C_{|\boldsymbol{x}(n)|} = 1 - CC_x$. In other words, the CCDF must satisfy the following

$$C_{|\boldsymbol{x}(n)|} = \Pr\{\text{PAPR} > \text{PAP}R_0\} \tag{6}$$

where $\text{PAP}R_0$ is the desired PAPR value which we shall use interchangeably with γ in this study.

A. ICF

The ICF algorithm [10] clips the amplitude of $x(n)$ to a threshold say T if the amplitude, $|\boldsymbol{x}(n)|$, exceeds T. This can be expressed as

$$\hat{\boldsymbol{x}}(n) = \begin{cases} T \times \exp(j \times \theta_n), & |\boldsymbol{x}(n)| > T \\ \boldsymbol{x}(n) & otherwise \end{cases} \tag{7}$$

where $j = \sqrt{-1}$, $\hat{\boldsymbol{x}}(n)$ represents the resulting clipped OFDM signal and $\theta_n = \arg\{\boldsymbol{x}(n)\}$ is the phase of $\boldsymbol{x}(n)$. The clipping is subject to a clipping ratio that can be described as [8]

$$T = \gamma \times \sqrt{P_{av}} \tag{8}$$

where γ is the clipping ratio and $P_{av} = \frac{1}{LN}\sum_n |\boldsymbol{x}(n)|^2$ is the average power of the OFDM signal before the clipping. The side-effect of clipping OFDM signals is that it leads to in-band distortion with out-of-band emission from oversampling. In Fig. 1, a typical ICF technique is depicted. The architecture involves iteratively clipping and filtering of excess signals up to the number of desired iterations until a required PAPR value is attained. Notice that the clipping ratio is a fixed parameter; this will be revisited and discussed, later, in Section II-C.

B. OICF AND SOICF

The process of iteratively clipping and filtering OFDM signals expends the energy of the system in the order of the iterations [11]. A way to circumvent this problem is to deploy an optimal filter construction technique that enables the ICF to converge quickly while achieving the optimum possible PAPR reduction. Thus, recall the PAPR relation stated in (4), Wang and Luo [4] have shown that it is possible to achieve a target PAPR with reduced iterations by using an optimal filter. For example, they used CVX optimization technique to construct a filter envelope for reducing out-of-band emission during ICF PAPR reduction. It involves the translation of the conventional PAPR equation to a convex problem so that the CVX optimization method can be applied. Now, let the PAPR problem be also expressed as [4], [8]

$$\textbf{PAPR} = \frac{\max\limits_{n=0,1,\cdots,lN-1}\left(|x(n)|^2\right)}{\frac{1}{lN}\sum\limits_{n=0}^{lN-1}\left(|x(n)|^2\right)} = \frac{\|\boldsymbol{x}\|_\infty^2}{\frac{1}{LN}\|\boldsymbol{x}\|_2^2} \tag{9}$$

where $\|\cdot\|_\infty = \max(|x(0)|, |x(1)|, \cdots, |x(LN-1)|)$ and $\|\cdot\|_2 \leq \left(\sum|\cdot|^2\right)^{\frac{1}{2}}$. In the conventional ICF, a rectangular

window ($\mathcal{G}$) is set to filter the out-of-band spectral regrowth with little concern on the consequential effects of the IFFT processing [4]. Put differently, the filter envelope requires many clipping-filtering iterations to attain the required PAPR value. The filter can be expressed as

$$\mathcal{G} = \begin{cases} 1 & 0 \leq n \leq N-1 \\ 0 & N \leq n \leq LN-1 \end{cases} \tag{10}$$

The rectangular window filter $\mathcal{G}$ does not maximize the desired PAPR at each iteration, m; $\forall m = 1, 2, \cdots, M$. One of the ways of solving this problem is by setting the following optimal conditions that are defined based on minimizing the EVM under certain conditions (listed in [4] and [8]) such as

$$\min_{\mathcal{G}_m \mathbb{C}^N} \mathbf{EVM} = \frac{\|X - C_m\|_2}{\|X\|_2} \tag{11a}$$

subject to

$$C_m = C_m^I \bullet \mathcal{G} \tag{11b}$$

$$C_m^o = 0 \tag{11c}$$

$$\boldsymbol{x}_{m+1} = IDFT\left(\bar{C}_m\right) \tag{11d}$$

$$\frac{\|\boldsymbol{x}_{m+1}\|_\infty}{\|\boldsymbol{x}_{m+1}\|_2 / \sqrt{LN}} \leq \sqrt{PAPR_{max}} = \gamma \tag{11e}$$

where C_m and C_m^I are the inband components, C_m^o is the out-band component such that $\bar{C}_m = \left[C_m; C_m^o\right]$ in the frequency domain and $\bullet$ represents element-wise multiplication. **EMV** represents the error vector magnitude whose root-mean-square is used to measure the degree of distortion suffered by OFDM signals after clipping and can be defined as

$$\xi = \frac{1}{\sqrt{N}} \left(\sum_{i=1}^{N} \mathbf{EMV}_i \right)^{\frac{1}{2}} \tag{12a}$$

From (11), $\|X - C_m\|_2$ must be kept reasonably small for the system to exhibit good BER performance. We seek a construction or solution PAPR vector that can reduce the noise instead of designing a filter that can constrain the peak amplitudes of the OFDM symbol. Meanwhile, the constraint function in (11e) is not convex and can be transformed to assume convexity as follows [4]

$$\|\boldsymbol{x}_{m+1}\|_\infty \leq \frac{1}{\sqrt{LN}} \left\|\hat{\boldsymbol{x}}_m\right\|_2 \gamma \tag{13}$$

where the RHS of (13) is the new optimal approximate clipping level, $\hat{\boldsymbol{x}}_m$ is the m^{th}-symbol immediately after clipping (time domain).

Simplify $\alpha = \frac{\|X - C_m\|_2}{\|X\|_2}$, then the optimization problem can be reformulated as

$$\min_{\mathcal{G}_m \in \mathbb{C}^N, \alpha \in \mathbb{R}} \quad \alpha \tag{14a}$$

subject to

$$\boldsymbol{x}_{m+1} = IDFT\left(\bar{C}_m\right) \tag{14b}$$

$$\|\boldsymbol{x}_{m+1}\|_\infty \leq \gamma \frac{\|\bar{\boldsymbol{x}}_m\|_2}{\sqrt{LN}}. \tag{14c}$$

Different problems surround the convex optimization problem of (14); for example, it involves running a special public software namely CVX [13] to construct the optimal solution filter which further expends the OFDM system power and expands the processing time in addition to the existing processing costs of driving the FFT/IFFT blocks demonstrated in [11]. To overcome this problem, the convex optimization can be reformulated and solved using the LMO technique by substituting PAPR reducing vector in (14). Let $W = X - C_m$ be the noise vector realized after each clipping operation, then (11) can be rewritten as

$$\min_{W_m \in \mathbb{C}^N} \mathbf{EVM} = \frac{\|W_m\|_2}{\|x\|_2} \tag{15a}$$

$$subject\ to\ \boldsymbol{w}_{(m+1)} = IDFT\left(W_m\right) \tag{15b}$$

$$\left|\boldsymbol{x}_{(m+1)} - \boldsymbol{w}_{(m+1)}\right| \leq \gamma \frac{\|\bar{\boldsymbol{x}}_m\|_2}{\sqrt{LN}}. \tag{15c}$$

Notice that $\left\|\hat{\boldsymbol{x}}_m\right\|_2$ of (13) is now replaced with $\|\bar{\boldsymbol{x}}_m\|_2$ in (15c) which approximates $\|\boldsymbol{x} - \boldsymbol{w}\|_2$ to achieve convex criteria in time domain, where $\boldsymbol{w} = IDFT(W)$. Now, squaring both sides redefine (14) as follows

$$\min_{W_m \in \mathbb{C}^N} \alpha^2 = \frac{\|W_m\|_2^2}{\|X\|_2} \tag{16a}$$

subject to

$$|\boldsymbol{x}_m - \boldsymbol{w}_{m+1}|^2 \leq \frac{\gamma^2 \|\bar{\boldsymbol{x}}_m\|_2^2}{\sqrt{LN}} \tag{16b}$$

where $\boldsymbol{w}_{m+1} = \text{IFFT}\,(W)_{1 \times LN}$.

The major difference between OICF and SOICF is that while OICF uses filter coefficients (in other words optimal $\mathcal{G}$) as the optimization parameter, while SOICF uses additive-PAPR vector. Now, denote the Lagrange function for the problem (16) as $\mathcal{L}(W_m, \lambda)$ for problem (14), then

$$\mathcal{L}(W_m, \lambda) = \frac{\|W_m\|_2^2}{\|X\|_2^2} + \lambda \left(|\boldsymbol{x}_m - w_{m+1}|^2 - \frac{\gamma^2 \left\|\hat{\boldsymbol{x}}_m\right\|_2^2}{\sqrt{LN}} \right) \tag{17}$$

where λ is the Lagrange multiplier. Similar problems have been solved in [8] and [20] using Karush-Kuhn-Tucker (KKT) discussed in [21]. Thus, based on the KKT conditions, the solution to (17) can be similarly found as [8]

$$W_m = \frac{1}{\sqrt{N}} \left(|x_m| - \frac{\gamma \|\bar{\boldsymbol{x}}_m\|_2}{\sqrt{LN}} \right) e^{j\theta_m} \tag{18}$$

where $\theta_m = \arg\{\boldsymbol{x}_m\}$ is the phase of $\boldsymbol{x}_m$.

C. ADAPTIVE SOICF TECHNIQUE

The theory of adaptive ICF has been discussed in the conventional non-optimized ICF was earlier presented in [14]. In this study, however, we extend the solution to an optimized ICF technique that does not have the computational complexities of [4] and non-optimized adaptivity of [14]. In Fig. 1, the conventional ICF architecture is shown from which the architectures for both OICF and the present SOICF

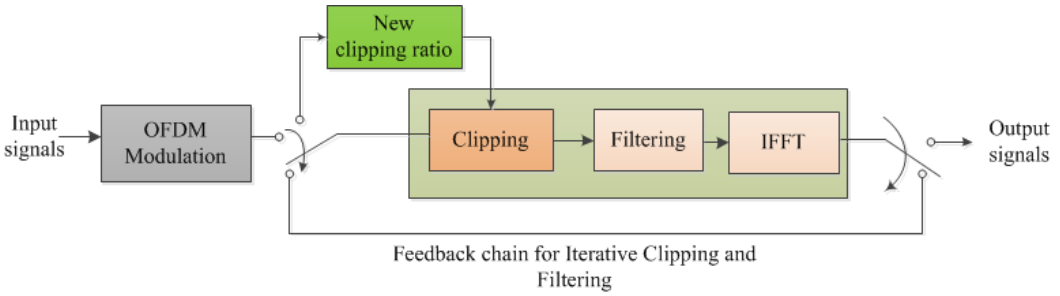

FIGURE 2. Proposed architecture for implementing adaptive SOICF based on an adaptively updated clipping threshold.

are derived. The problem with the traditional ICF is that the CR is constant, thus the clipping threshold is also constant. Since each iteration follows with a new set of amplitudes, it is best to reset the clipping threshold to respond to the prevailing amplitudes of the clipped signals. Consequently, we modify Fig. 1 to include new clipping ratio at each iteration as shown in Fig. 2.

It is worthy to emphasize here that in ICF, OICF and SOICF, a major problem is that since there is peak regrowth, there exists no compensation to balance out the resulting signal power; this unfairly leads to low BER measure (good BER performance) and does not exist in the proposed adaptive SOICF design. However, using (8), the solution (18) can be simplified as

$$W_m = \frac{1}{\sqrt{N}} \left(|x_m| - T_m^{'} \right) e^{j\theta_m} \tag{19}$$

where

$$T_m^{'} = \frac{\gamma \, \|\bar{\boldsymbol{x}}_m\|_2}{\sqrt{LN}} \tag{20}$$

is the newly updated clipping threshold at each iteration from recalculating γ. Thus, the optimal solution to both the convex optimization problem and the LMO problem (during implementation) reduces to constructing optimal threshold during each new iteration that solves (19). In closed form, the average EVM of an OFDM clipped signal can be expressed as a function of the clipping ratio such as [14]

$$\mathbb{E}\{\text{EVM}\} = \left\{ \exp\left(-\gamma^2\right) - \sqrt{\pi}\gamma \operatorname{erfc}(\gamma) \right\}^{\frac{1}{2}} \tag{21}$$

where $\mathbb{E}\{\cdot\}$ is the expectation value operator. From (21), it can be observed that the average EVM depends on the clipping ratio and this is depicted in Fig. 3. Notice that in Fig. 1 that clipping process is non-adaptive as the proposed in Fig. 2.

Given a reference maximum amplitude A_{max} of any OFDM signal frame, let us rewrite the the clipping ratio as [14]

$$\gamma = \frac{A_{max}}{A_{ave}} \tag{22}$$

where

$$A_{max} = \underset{0<n<LN-1}{\arg\max} \left\{ \left| \hat{\boldsymbol{x}}(n) \right| \right\} \tag{23}$$

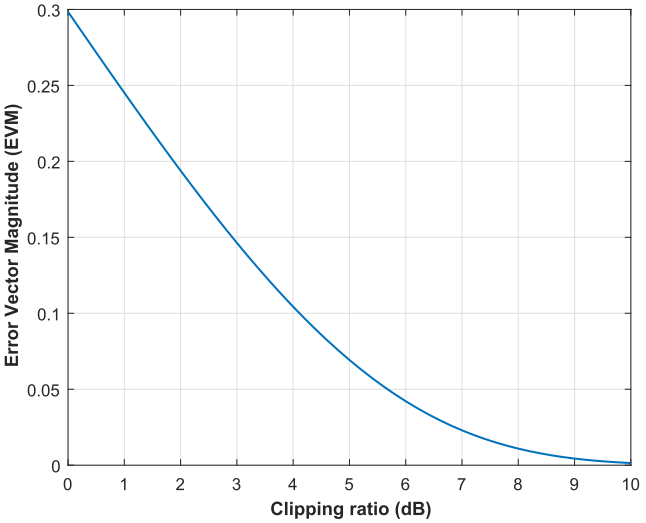

FIGURE 3. Effect of clipping ratio on the performance of average EVM; EVM directly affects the BER output performance of clipped OFDM signals.

$$A_{ave} = \frac{1}{LN} \sum_{n=0}^{LN-1} \left| \hat{\boldsymbol{x}}(n) \right| \tag{24}$$

A_{ave} is the average amplitude that now varies with each iteration and hasten attaining the PAPR target. It can be seen from Fig. 3 that EVM falls with increasing γ. This implies that for low values of γ, the EVM will be high since there are many peaks exceeding the average to be clipped. In [11], the clipping threshold has been expressed in closed form in relation to the CCDF of the PAPR associated with clipping and the number of subcarriers as

$$\gamma = -0.5\mathbb{L}_w \left(\frac{-6}{\pi N^2} \ln\left(1 - C_{|x|}\right)^2 \right) \tag{25}$$

where $\mathbb{L}_w(\cdot)$ represents the Lambert's W-function and $C_{|x|}$ is the CCDF from (6). If the clipping threshold is linked to the EVM performance, then the CCDF can also be discussed in terms of the clipping threshold given the number of subcarriers N and so on.

By substituting (25) into (21) for γ, we represent the performance of the CCDF and EVM for different subcarriers as in Fig. 4. It is observed that as the EVM increases, the

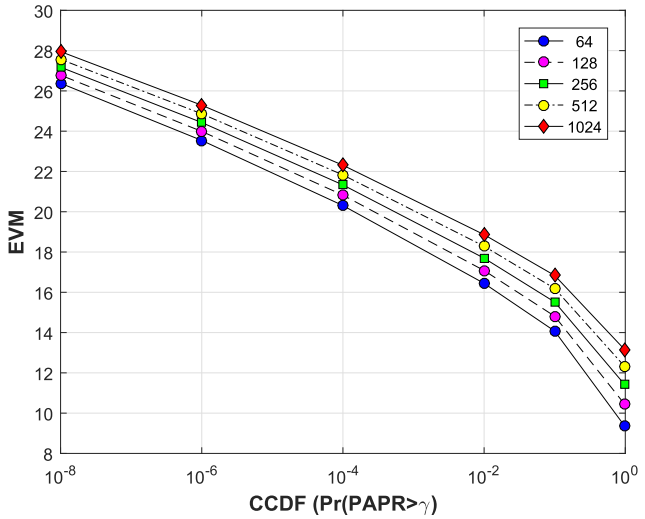

FIGURE 4. Effect of the error vector magnitude on the CCDF of an OFDM system given different number of subcarriers.

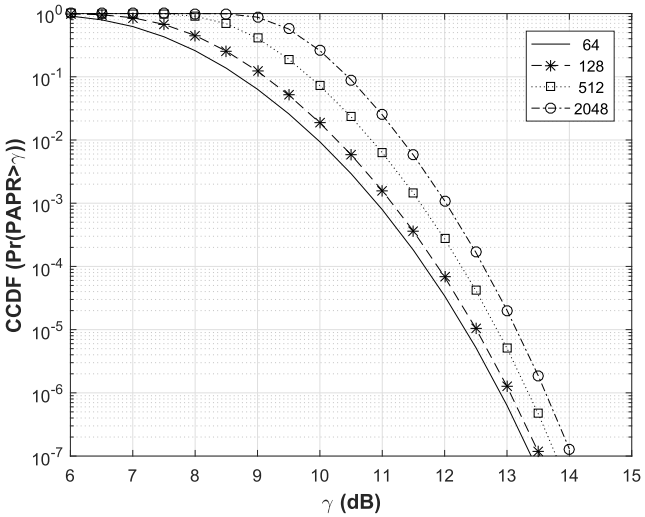

FIGURE 5. PAPR CCDF evaluation as a function of the clipping ratio based on Lambert's W-function for different OFDM subcarriers.

CCDF falls. It is also clear that for any given EVM, the CCDF performance improves as the number of subcarriers increases.

Although the worsens knowledge of PAPR performances with the target PAPR is well documented, we, nevertheless use (25) to confirm this. For example, considering the effects of the clipping threshold on the PAPR using (25), we demonstrate in Fig. 5 that the PAPR of OFDM system falls with decreasing N. Similar to the trend shown in Fig. 4, the PAPR CCDF also increases with increasing number of OFDM subcarriers as in Fig. 5.

Now, going back to Fig. 2 which has been inspired from the study of adaptive ICF reported in [14] although the architecture proposed in this study (Fig. 2) is quite improved and different, that study does not consider the optimal solution of PAPR reported in [4] nor the simplified version presented in [8]. However, since the LMO method provides a computationally efficient technique and better performance than OICF, the new optimal clipping ratio (shown in Fig. 2) is determined as follows

$$T'_{m,new} = \frac{\gamma \left\| \hat{\boldsymbol{x}}_m \right\|_2}{\sqrt{LN}} \tag{26}$$

From (26), there exists a new clipping threshold $T'_{m,new}$ at each new iteration based on the resulting clipped and filtered signal that updates (8) using (23) and (24).

As shown in Fig. 6, when CR is recalculated at each iteration, the average power of clipped signals drops after a few iterations, which indicates peak regrowth is better handled compared to using a static parameter based on a preset CR and $|\boldsymbol{x}(n)|$.

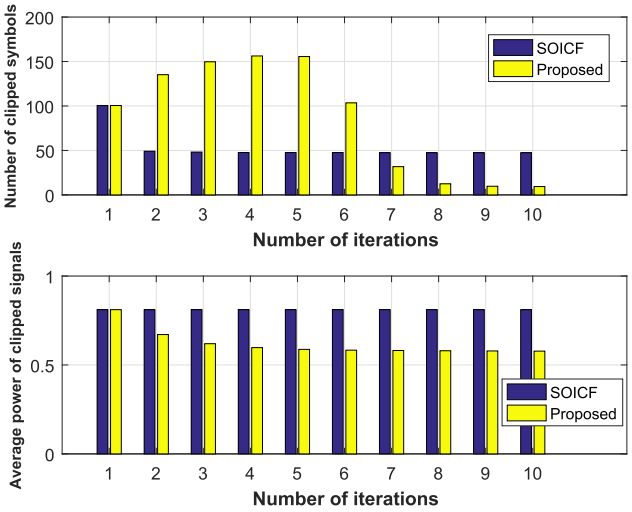

FIGURE 6. Comparison of number and the power of clipped signals at different iterations for conventional SOICF and proposed adaptive SOICF ($\gamma = 2.10$ dB).

From Fig. 6, it can be observed that the number of clipped signals falls to standstill after the first clipping and remains constant with the number of iteration in the case of conventional SOICF method discussed in [8]. This implies that the PAPR reduction capability attains its minimum possible after the first few iterations. Also, since the determining amplitude is fixed, the new amplitude that exceeds a threshold is not newly measured with respect to all other amplitudes even if they all approach a uniform distribution. However, in the proposed method, the number of amplitudes clipped at each iteration is strictly a function of the rest amplitudes (not fixed). This accounts for why in this scheme high number of amplitudes are clipped between the second and the sixth iteration (unlike the conventional SOICF) and falls sharply at the subsequent iteration. Also, even after the conventional SOICF reaches its optimum point of operation, more symbols are clipped in the proposed SOICF (due to the use of an adaptive clipping threshold), which clearly demonstrates the limited capability of the conventional scheme. The trend in Fig. 6 is also confirmed by Fig. 7 although both techniques exhibited peak clipping at the second and third iterations.

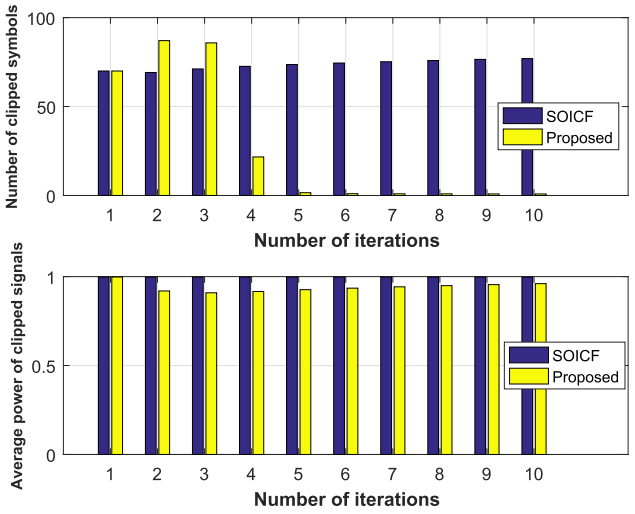

FIGURE 7. Comparisons for number and the power of clipped signals at different iterations for conventional SOICF and proposed adaptive SOICF ($\gamma = 3$ dB).

In addition, we also measure the average power of the clipped signals (for $\gamma = 2.10$ and 3 dB) as shown in Figs. 6 and 7 (respectively). The clipping ratio determines the output power. The proposed adaptive SOICF technique shows a different trend to the power and amplitudes of the clipped signals than the ones in SOICF. Since the clipping threshold tends to vary (for the adaptive), the PAPR drops more compared to the conventional SOICF (with a fixed threshold) which confirms the theoretical illustrations in Figs. 5, 4 and 3 as well as (25) and (21). For the proposed SOICF, it follows that at all clipping ratios and the power of the clipped signals respond to the peak regrowth. Notice also that the power of clipped signals is higher in Fig. 7 than in Fig. 6 due to the preset clipping ratio for both SOICF and the proposed adaptive SOICF.

Algorithm 1 Proposed PAPR Reduction Algorithm

- **Initialization:** Set the desired clipping threshold T and set the number of iterations M
- **Step 1:** Construct and scale $\mathcal{G}$ as $\mathcal{G} = \left[1, 1, \cdots 1_N, 0, 0, \cdots, 0_{N(L-1)}\right]/\sqrt{N}$
- **Step 2:** Compute the clipping threshold according to (8)
- **Step 3:** Compute the error vector as $V_m = (|x_m(n)| - T_m)\, e^{j \arg\{x_m(n)\}}$
- **Step 4:** Convert V_m to frequency domain
- **Step 5:** Multiply $\mathbf{V}_m$ by $\mathcal{G}$ as $D_f = \mathbf{V}_m \times \mathcal{G}$
- **Step 6:** Convert D_f into time domain as $d_t = ifft\left(D_f\right)$
- **Step 7:** Obtain the PAPR reduced signal as $x_{m+1} = x_m - d_t$
- **Step 8:** Update T_m according to (26) or transmit if the desired iteration/target has been reached.

In Algorithm 1, we demonstrate step-by-step procedure on how to implement the proposed adaptive SOICF PAPR reduction scheme. Given a chosen clipping ratio, T can be calculated as in (8) and M is the maximum number of iterations such that $1 \leq m \leq M$. Following the steps 1 - 8, the signal is transmitted if the target PAPR is achieved or T is updated at each iteration based on the resulting measure of the average amplitude of the OFDM signal.

III. PERFORMANCE EVALUATION OF ADAPTIVE SOICF AND THE CONVENTIONAL SOICF

In this section, we report the performance of the proposed adaptive SOICF through simulation for different scenarios. The simulation involves $N = 128$ randomly generated input signals that are modulated using the quadrature phase shift keying (QPSK). The QPSK output symbols are then oversampled by $L = 4$ so that a total of 512 IFFT/FFT block is used. To realize the time domain signals, $\boldsymbol{x}(n)\ \forall n = 0, 1, \cdots, LN-1$ as represented in (1), we drive the QPSK modulated input symbols using an over-sized $LN-$IFFT block. We estimated the amplitude of the signals and compared them with the set/desired amplitude threshold, T, and then clipped off the excess amplitudes. The resulting signals are then converted into frequency domain to enable the filtering of the out-of-band components. Since this causes peak regrowth, we process the output over many iterations in order to reduce the PAPR and prevent the power amplifier from operating near the saturation region. In a way, PAPR reduction techniques tend to bring the distribution of OFDM signal amplitudes peaks towards a uniform distribution. After the third iteration, we exit the process and convert the frequency domain signals into time-domain signals for transmission and measure the PAPR of which are reported in the following subsection. The received signal at the receiver can be expressed linearly as $\boldsymbol{y}(n) = \boldsymbol{x}(n) + \boldsymbol{z}(n)$, where $\boldsymbol{z}(n) \sim \mathcal{N}(0, \sigma_z^2)\ \forall n = 0, 1, \cdots, LN-1$ is the additive white Gaussian noise and $\boldsymbol{z} \sim \mathcal{N}(\psi, \sigma_x^2)$ suggests that $\boldsymbol{z}$ is Gaussian variable identically and independently distributed with mean ψ and variance σ_z^2. The received signal is then converted back to frequency domain and the oversampling is removed. At the output of the QPSK demodulator, the bit values for received signals are extracted and compared to the originally transmitted information bits to calculate the BER as shown in in Section III-B.

A. PAPR EVALUATION

In this subsection, we compare the performance of the proposed optimization of SOICF with the conventional SOICF technique. It involves simulations for three iterations involving clipping and filtering. In Fig. 8, we find that SOICF significantly reduces the original PAPR, and converges around 7dB. On the other hand, the clipping ratio target PAPR (dB) is 2.10dB which the SOICF does not achieve with 3 iterations. In the case of the adaptive technique, the 3dB target is achieved with 3 iterations thus saving the costs of driving the IFFT/FFT blocks beyond 3 iterations.

Furthermore, since PAPR varies with the number of FFT block deployed, we investigate a design that uses 128-symbol block size with an oversampling factor of $L = 4$. From Fig. 9, we see that the proposed adaptive SOICF attains the target PAPR threshold faster than the conventional

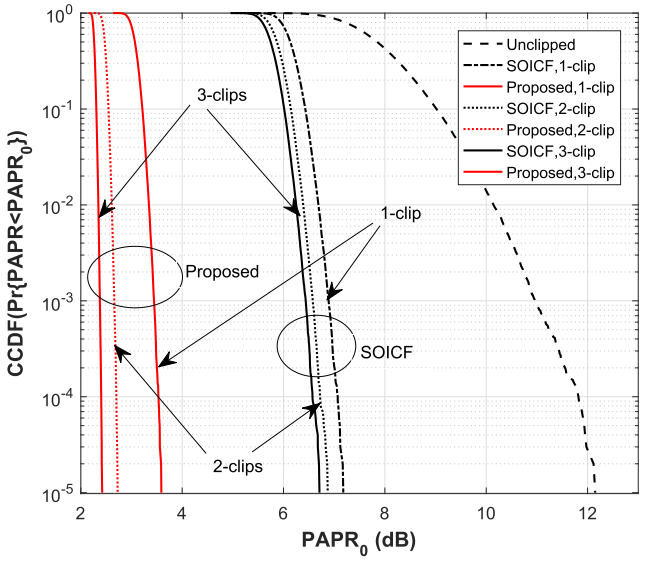

FIGURE 8. PAPR performance evaluation of the proposed adaptive SOICF (labeled as Proposed) and the conventional SOICF using the following parameters $N = 128$, $L = 4$, $\gamma = 2.10$ dB.

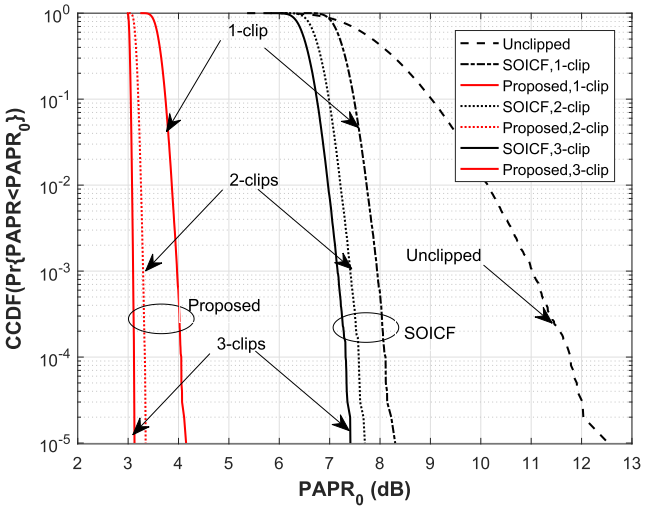

FIGURE 9. PAPR performance evaluation of the proposed adaptive SOICF (labeled as Proposed) and the conventional SOICF using the following parameters $N = 128$, $L = 4$, $\gamma = 3$dB.

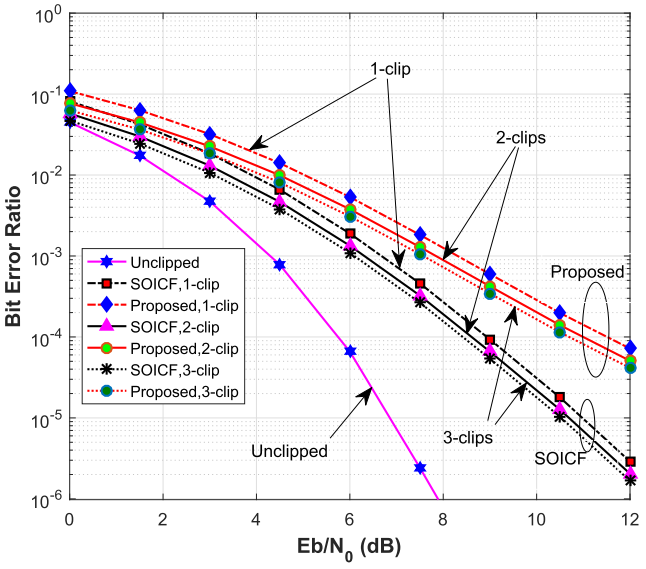

FIGURE 10. BER performance evaluation of the proposed adaptive SOICF and conventional SOICF ($L = 4$, $N = 128$, $\gamma = 2.10$dB).

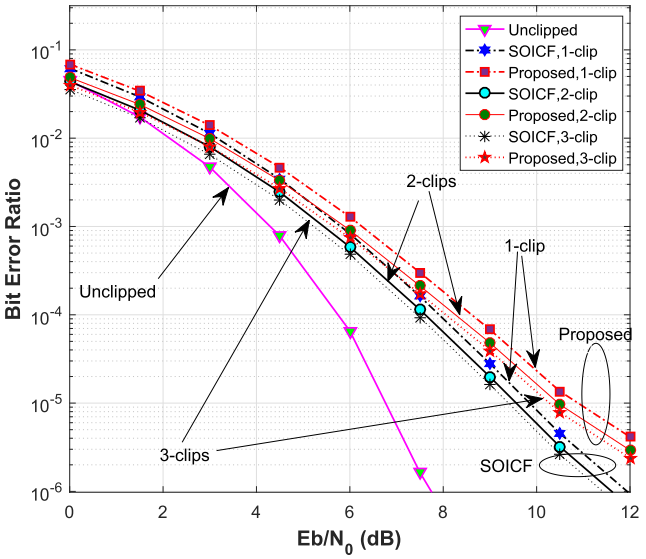

FIGURE 11. BER performance evaluation of the proposed adaptive SOICF and conventional SOICF ($L = 4$, $N = 128$, $\gamma = 3$dB).

SOICF. Thus, our method saves the cost of expending the device resources to drive the IFFT/FFT blocks through more iterations.

For practical system implementations and industrial applications, it can be advised that the proposed technique may not necessarily need to be applied beyond a certain number of iterations to minimize the cost of driving the FFT/IFFT blocks if a target amplitude has already been reached.

B. BER PERFORMANCES

Although the BER performances were not discussed in [14], in this section, we evaluate them for the conventional SOICF technique as well as the proposed method. In Fig. 10, we observe that the performance of the proposed technique is worse than the conventional SOICF, as the channel conditions deteriorate (i.e. $E_b/N_0 < 6$ dB).

Similar to the result described in Fig. 10, we also observe a similar trend in Fig. 11. The key difference in Fig. 11 is that the BER performance gap between the conventional and the proposed schemes is narrow even at $E_b/N_0 > 8$ dB range, which is attributed to the increased clipping level from 2.1 to 3 dB. (This finding is also confirmed by Fig. 13, as will be explained shortly).

C. PAPR AND BER PERFORMANCES FOR DIFFERENT CLIPPING RATIOS

For ease of parametric assessment and selections, we present the performances of different CRs using the conventional and the proposed SOICF PAPR reduction techniques. In Fig. 12,

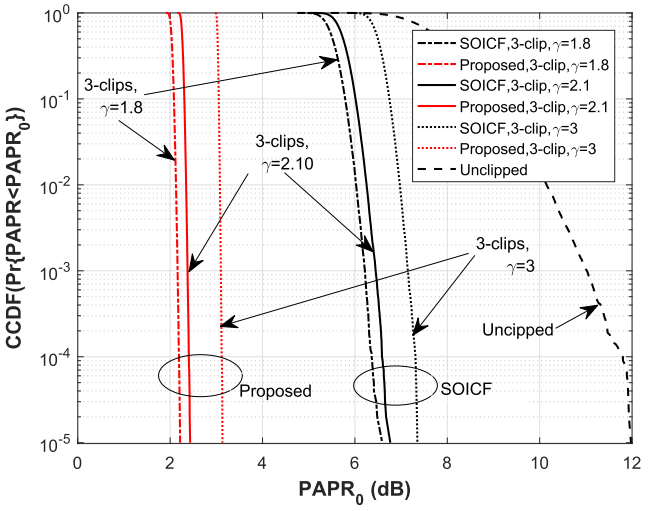

FIGURE 12. PAPR performance comparison of the proposed adaptive SOICF with conventional SOICF for different clipping levels ($\gamma = 1.8$, 2.10 and 3 dB, $L = 4$, $N = 128$).

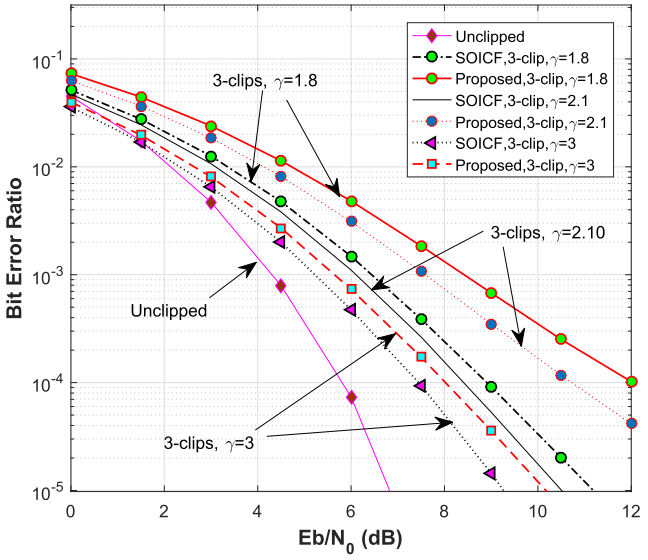

FIGURE 13. BER performance comparison of the proposed adaptive SOICF with conventional SOICF for different clipping levels ($\gamma = 1.8$, 2.10 and 3dB, $L = 4$, $N = 128$).

the PAPR performances for the proposed adaptive SOICF and the conventional SOIC were iteratively clipped and filtered three times before transmission occurs. Clearly, it can be seen that proposed adaptive PAPR reduction technique outperforms the conventional SOICF at all clipping ratios, at least by 3 dB at each instance. Notably, as the clipping ratio is reduced, the proposed technique outperforms the conventional SOICF. For example, in the case of $\gamma = 1.8$ dB, the proposed adaptive SOICF technique performs 4.5dB better than the conventional SOICF and so on. Our findings prove the effectiveness of the adaptive estimation in terms of achieving a target PAPR and confirm the illustrations in Section II-C.

Next, we present the BER performances for the two PAPR techniques (i.e. SOICF and adaptive SOICF) as shown in Fig. 13. It is found that BER performance of the proposed adaptive SOICF approaches that of the conventional SOICF as the clipping thresholds get smaller. For large clipping levels, since the BER degradation is minimal, the proposed technique can be upheld for ensuring good BER performance at a desired PAPR level at minimal processing cost.

IV. CONCLUSION

In this study, an improvement to the optimization of iterative clipping and filtering process of OFDM signals has been presented. The core concept is to adaptively optimize the iterative clipping and filtering of OFDM signals to reduce design complexity and processing resource usage with a BER performance tradeoff. The study has extended the earlier simplified optimization of ICF that eliminates the dependency on a special optimization software (namely CVX) to construct optimal filters. Based on Lagrange multiplier optimization process, a simpler solution which reduces the number of iterations required to attain a desired clipping threshold has been presented. By adaptively resetting the clipping threshold, instead of the conventional method of using a hard/fixed-clipping threshold, a faster convergence to a desired clipping level and thus a required PAPR has been achieved. Although the BER performance of the proposed adaptive SOICF approaches to that of the conventional SOICF at higher clipping ratios, the PAPR gain of the adaptive method is significantly better at all clipping ratios. We have also presented the theoretical performance benchmarks and the mathematical framework related to this study for completeness.

REFERENCES

[1] S. Weinstein and P. Ebert, "Data transmission by frequency-division multiplexing using the discrete Fourier transform," *IEEE Trans. Commun. Technol.*, vol. 19, no. 5, pp. 628–634, Oct. 1971.
[2] Y. Rahmatallah and S. Mohan, "Peak-to-average power ratio reduction in OFDM systems: A survey and taxonomy," *IEEE Commun. Surveys Tuts.*, vol. 15, no. 4, pp. 1567–1592, 4th Quart., 2013.
[3] K. O. O. Anoh, R. A. Abd-Alhameed, J. M. Noras, and S. M. R. Jones, "Wavelet packet transform modulation for multiple input multiple output applications," *Int. J. Comput. Appl.*, vol. 63, no. 7, pp. 46–51, Feb. 2013.
[4] Y.-C. Wang and Z.-Q. Luo, "Optimized iterative clipping and filtering for PAPR reduction of OFDM signals," *IEEE Trans. Commun.*, vol. 59, no. 1, pp. 33–37, Jan. 2011.
[5] J. Joung, C. K. Ho, K. Adachi, and S. Sun, "A survey on power-amplifier-centric techniques for spectrum- and energy-efficient wireless communications," *IEEE Commun. Surveys Tuts.*, vol. 17, no. 1, pp. 315–333, 1st Quart., 2015.
[6] G. Wunder, R. F. H. Fischer, H. Boche, S. Litsyn, and J.-S. No, "The PAPR problem in OFDM transmission: New directions for a long-lasting problem," *IEEE Signal Process. Mag.*, vol. 30, no. 6, pp. 130–144, Nov. 2013.
[7] H. Suraweera, K. Panta, M. Feramez, and J. Armstrong, "OFDM peak-to-average power reduction scheme with spectral masking," in *Proc. Int. Symp. Commun. Syst. Netw. Digit. Signal Process.*, 2004, pp. 160–163.
[8] X. Zhu, W. Pan, H. Li, and Y. Tang, "Simplified approach to optimized iterative clipping and filtering for PAPR reduction of OFDM signals," *IEEE Trans. Commun.*, vol. 61, no. 5, pp. 1891–1901, May 2013.
[9] V. Nandalal and S. Sophia, "PAPR reduction of OFDM signal via custom conic optimized iterative adaptive clipping and filtering," *Wireless Pers. Commun.*, vol. 78, no. 2, pp. 867–880, Sep. 2014.
[10] J. Armstrong, "Peak-to-average power reduction for OFDM by repeated clipping and frequency domain filtering," *Electron. Lett.*, vol. 38, no. 5, pp. 246–247, Feb. 2002.

[11] A. K. Gurung, F. S. Al-Qahtani, A. Z. Sadik, and Z. M. Hussain, "Power savings analysis of clipping and filtering method in OFDM systems," in *Proc. Australasian Telecommun. Netw. Appl. Conf. (ANTAC)*, Dec. 2008, pp. 204–208.
[12] A. K. Gurung, F. S. Al-Qahtani, A. Z. Sadik, and Z. M. Hussain, "One-iteration-clipping-filtering (OICF) scheme for PAPR reduction of OFDM signals," in *Proc. Int. Conf. Adv. Technol. Commun.*, Oct. 2008, pp. 207–210.
[13] M. Grant and S. Boyd. (Mar. 2017). *CVX: MATLAB Software for Disciplined Convex Programming, Version 2.1., Build 1116*. [Online]. Available: http://cvxr.com/cvx
[14] Y. Wang, W. Chen, and C. Tellambura, "Genetic algorithm based nearly optimal peak reduction tone set selection for adaptive amplitude clipping PAPR reduction," *IEEE Trans. Broadcast.*, vol. 58, no. 3, pp. 462–471, Sep. 2012.
[15] M. Wang and B. Xiao, "A PAPR reduction method based on differential evolution," *J. Commun.*, vol. 10, no. 6, pp. 435–441, Jun. 2015.
[16] C. Sharma, P. K. Sharma, S. K. Tomar, and A. K. Gupta, "A modified iterative amplitude clipping and filtering technique for PAPR reduction in OFDM systems," in *Proc. Int. Conf. Emerg. Trends Netw. Comput. Commun.*, 2011, pp. 365–368.
[17] Y. Wang, J. Ge, L. Wang, J. Li, and B. Ai, "Nonlinear companding transform for reduction of peak-to-average power ratio in OFDM systems," *IEEE Trans. Broadcast.*, vol. 59, no. 2, pp. 369–375, Jun. 2013.
[18] K. Anoh, R. Abd-Alhameed, Y. Dama, S. Jones, P. Pillai, and K. Voudouris, "An investigation of PMEPR of WPT-OFDM and OFDM multicarrier systems," *J. Commun. Netw.*, vol. 3, no. 3, pp. 45–52, 2013.
[19] Y. Rahmatallah, N. Bouaynaya, and S. Mohan, "On the performance of linear and nonlinear companding transforms in OFDM systems," in *Proc. Wireless Telecommun. Symp. (WTS)*, Apr. 2011, pp. 1–5.
[20] K. Wu, G. Ren, and M. Yu, "PAPR reduction of SC-FDMA signals using optimized additive pre-distortion," *IEEE Commun. Lett.*, vol. 19, no. 8, pp. 1446–1449, Aug. 2015.
[21] S. Boyd and L. Vandenberghe, *Convex Optimization*. Cambridge, U.K.: Cambridge Univ. Press, 2004.

KELVIN ANOH (S'11–M'15) received the B.Sc. degree (Hons.) in Industrial Physics from Ebonyi State University, Nigeria, in 2006, the M.Sc. degree in Data Telecommunications and Networks from the University of Salford, U.K., in 2010, and the Ph.D. degree in Telecommunications Engineering from the University of Bradford, U.K., in 2015. Since 2016, he has been with Manchester Metropolitan University, U.K., as a Post-Doctoral Research Fellow. He has authored many peer-reviewed papers in signal processing. His research interests include signal processing and emerging communication technologies. He is a member of the IET. He graduated as the best student in the department and received the Ebonyi State Government fully sponsored Scholarships for M.Sc. and Ph.D. studies simultaneously as one of the best in the University. At MMU, he worked on the joint Innovate UK - EPSRC project on Smart In-Building Micro-Grid for Energy Management which received both the Knowledge Exchange Project Award–Winner and Outstanding knowledge Award–Winner of 2016.

CAGRI TANRIOVER received the B.Sc. degree in electronics and communications engineering from Istanbul Technical University in 1997, and the M.Sc. degree in digital signal processing and the Ph.D. degree in communications systems from Lancaster University, U.K. He has an extensive industrial research and product development experience of over 14 years as part of multidisciplinary teams in the U.K., Turkey, and the USA. He has successfully contributed to ETSI's TETRA TEDS Release 2 Standard. He is the Co-Inventor of the multifold turbo coding technique, and has published a number of articles in peer reviewed journals and authored a number of international patents. His research interests include wireless communication, signal processing, and embedded systems.

BAMIDELE ADEBISI (M'06–SM'15) received the bachelor's degree in electrical engineering from Ahmadu Bello University, Zaria, Nigeria, in 1999, and the master's degree in advanced mobile communication engineering and the Ph.D. degree in communication systems from Lancaster University, U.K., in 2003 and 2009, respectively. He was a Senior Research Associate with the School of Computing and Communication, Lancaster University, from 2005 to 2012. He joined Manchester Metropolitan University, Manchester, in 2012, where he is currently a Reader in electrical and electronic engineering. He has been involved in several commercial and government projects focusing on various aspects of wireline and wireless communications. He has several publications and a patent in the research area of data communications over power line networks and smart grid. His research interests include the research and development of communication technologies for electrical energy monitoring/management, transport, water, critical infrastructures protection, home automation, IoTs, and Cyber Physical Systems. He is a member of the IET.